



## Increasing forest carbon sinks in cold and arid northeastern Tibetan Plateau

Zongying Cao<sup>a,b</sup>, Junzhou Zhang<sup>a,b,\*</sup>, Xiaohua Gou<sup>a,b,\*</sup>, Yuetong Wang<sup>a,b</sup>, Qipeng Sun<sup>a,b</sup>, Jiqin Yang<sup>a,b,c</sup>, Rubén D. Manzanedo<sup>d</sup>, Neil Pederson<sup>e</sup>

<sup>a</sup> Key Laboratory of Western China's Environmental Systems (Ministry of Education), College of Earth and Environmental Sciences, Lanzhou University, Lanzhou 730000, China

<sup>b</sup> Gansu Liancheng Forest Ecosystem Field Observation and Research Station, Lanzhou University, Lanzhou 730333, China

<sup>c</sup> Liancheng National Nature Reserve in Gansu, Lanzhou 730300, China

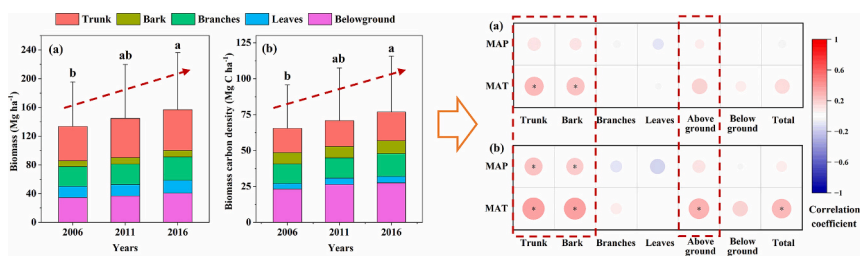
<sup>d</sup> Plant Ecology, Institute of Integrative Biology, D-USYS, ETH-Zürich, 8006 Zürich, Switzerland

<sup>e</sup> Harvard Forest, Harvard University, Petersham, MA 01366, USA

### HIGHLIGHTS

- 104-plot of forest inventories at three-phase were carried out at cold-arid regions.
- Spruce carbon density increased by 17.34 % from 2006 to 2016 in the Qilian Mountains.
- Warming and increasing precipitation contributed to the increase of carbon density.
- Carbon density increased while sequestration rate decreased with forest age.

### GRAPHICAL ABSTRACT



Increase of biomass and carbon density of spruce during the three inventory periods and their climatic impacts on the Qilian Mountains

### ARTICLE INFO

Editor: Kuishuang Feng

#### Keywords:

Biomass  
Carbon density  
Carbon stock  
Forest inventory  
Qinghai spruce  
Cold and arid regions

### ABSTRACT

Arid forest lands account for 6 % of the world's forest area, but their carbon density and carbon storage capacity have rarely been assessed. Forest inventories provide estimates of forest stock and biomass carbon density, improve our understanding of the carbon cycle, and help us develop sustainable forest management policies in the face of climate change. Here, we carried out three forest inventories at five-year intervals from 2006 to 2016 in 104 permanent sample plots covering the Qinghai spruce (*Picea crassifolia*) distribution in the north slope of Qilian Mountains, northeastern Tibetan Plateau. Results shows that mean biomasses for Qinghai spruce were 133.80, 144.89, and 157.01 Mg ha<sup>-1</sup> while biomass carbon densities were 65.52, 70.92, and 76.88 Mg C ha<sup>-1</sup>, in 2006, 2011, and 2016, respectively. This shows an increase in the Qinghai spruce carbon density of 17.34 % from 2006 to 2016. Both the precipitation and temperature play crucial roles on the increase of aboveground carbon density. The average carbon densities were different among forests with different ages and were higher for older forests. Our results show that the carbon sequestration rate for Qinghai spruce in the Qilian Mountains is significantly higher than the average rates of national forest parks in China, suggesting that this spruce forest has the potential to sequester a significant amount of carbon despite the general harsh growing conditions of cold and arid ecoregions. Our findings provide important insights that are helpful for the assessment of forest carbon for cold and arid lands.

\* Corresponding authors at: Key Laboratory of Western China's Environmental Systems (Ministry of Education), College of Earth and Environmental Sciences, Lanzhou University, Lanzhou 730000, China.

E-mail addresses: [zhangjz@lzu.edu.cn](mailto:zhangjz@lzu.edu.cn) (J. Zhang), [xhgou@lzu.edu.cn](mailto:xhgou@lzu.edu.cn) (X. Gou).

<https://doi.org/10.1016/j.scitotenv.2023.167168>

Received 24 April 2023; Received in revised form 21 August 2023; Accepted 15 September 2023

Available online 18 September 2023

0048-9697/© 2023 Elsevier B.V. All rights reserved.

## 1. Introduction

As one of the most important carbon pools in the world (Gibbs et al., 2007; FAO, 2020), forests account for 50–60 % of terrestrial ecosystems and absorb about 18 % of global CO<sub>2</sub> emissions (Pan et al., 2011; Friedlingstein et al., 2020). The dynamics of these systems can have a substantial impact on atmospheric CO<sub>2</sub> concentrations (O'Sullivan et al., 2019; Smith et al., 2014). Arid and semiarid regions are among the world's most fragile areas and occupy nearly 30 % of the world's land surface (Abdelhak, 2022; Wang et al., 2014). Arid forest land accounts for 6 % of the world's forest area and is important for arid zone ecosystems because it helps to maintain conditions that are suitable for agriculture, rangeland management and other human activities (Malagnoux, 2007). The social, economic, and environmental role of forests in arid lands is significant, despite their limited extent, and trees have often been used for sand dune fixation programs, windbreaks, erosion control, microclimate mitigation, and soil fertility restoration (Malagnoux, 2007). Arid forest land is an important part of the global and regional land carbon pool (Houghton, 2005; Fang et al., 2014; Le Noë et al., 2020; Zhao et al., 2021). Given the ongoing and projected warming and changes to drought regimes, further assessment into the carbon sequestration and storage capacity of forests in arid regions is needed to inform forest management and ecosystem services.

Biomass inventories, micrometeorological observations, and remote sensing simulations are the main methods used to study carbon storage and balance for forest ecosystems (Fang et al., 2018; Lu et al., 2018; Liu et al., 2019; Houghton, 2020; Zhang et al., 2022). Remote sensing, vorticity, and other modern technologies are often used to study spatial patterns of forest biomass (Gil et al., 2011; Xu et al., 2014), however these methods rely on site-measurements of biomass or carbon storage data and a sufficient amount of data to provide background parameters. Field surveys therefore remain one of the more reliable and widely used means of studying biomass and carbon density because they provide continuous and systematic data over large region (Fang et al., 1998; Nabuurs et al., 2003; Piao et al., 2005; Woodbury et al., 2007; Kindermann et al., 2008; Piao et al., 2009; Zhang et al., 2013; Fang et al., 2014; Zhang et al., 2015; Zhao et al., 2019; Gómez-García, 2020).

China is the world's largest energy consumer and carbon emitter (Zhou et al., 2014; Liu et al., 2016), but has been working at global climate governance. China is aiming to address climate change by increasing forest stock and has announced intentions to increase its to global climate-change mitigation through policies and measures such that peak carbon emissions is reached by 2030. The long-term goal is to achieve carbon neutrality by 2060. Accurate assessment of arid forest carbon sinks, which account for more than one third of China's land area, is an important part in understanding the contribution of forest carbon sinks to China's carbon goals.

The Qilian Mountains, a representative mountainous region in a continental climatic zone on the northeastern Tibetan Plateau (Wagner et al., 2015), are considered broadly cold and arid region. Accordingly, there is a variety of forest vegetation types and performs a range of ecological functions, such as soil and water conservation, carbon fixation, oxygen release, and species protection (Yang et al., 2022). Qinghai spruce (*Picea crassifolia* Kom., hereafter spruce) is the dominant tree species and is widely distributed throughout the coniferous forests of the region. Research has shown that the vegetation in the Qilian Mountains is highly sensitive to climate change (Xia et al., 2017; Chang et al., 2014). Some few studies have focused on spruce carbon density and storage there, but only at a single site (Wagner et al., 2015; Zhao et al., 2020). As far as we know, there are no reported studies of biomass and carbon storage over a large area like the climatically and ecologically dynamic Qilian Mountains region.

We carried out a three-phase forest inventory of above- and below-ground biomass at five-year intervals from 2006 to 2016 covering the range of spruce areas in the Qilian Mountains to analyze spruce carbon density and storage. We hypothesize that spruce carbon density and

storage is likely to be very low compared with the mean levels of national forest parks in China and other regions due to the cold and arid environmental conditions. We expect that the increase of the above-ground carbon density will be strongly related to increasing temperature and precipitation in this cold and arid region. Our study will be helpful for understanding changes in forest productivity. We hope to provide a theoretical basis for rational forest management policies in cold and arid regions.

## 2. Materials and methods

### 2.1. Study region

The hydrothermal conditions and complex topography in the Qilian Mountains result in different vegetation types that are distributed in distinct vertical zones (Fu et al., 2020; Qian et al., 2020; J.Z. Zhang et al., 2020). Most forests are on the east and middle elevations of the Qilian Mountains. The forest types are relatively simple in the Qilian Mountains, with pure forest of spruce on south-facing slopes and Qilian Juniper (*Juniperus przewalskii* Kom.) on north-facing slopes, and spruce accounted for >80 % of the forest area. Spruce is the endemic and dominant tree species and is widely distributed on shady or semi-shady slopes between 2600 and 3800 m above sea level (asl) in the eastern and central of the Qilian Mountains.

### 2.2. Forest inventories

Forest inventories were systematically conducted on 104 permanent plots in spruce forests on northern slopes across the central and eastern Qilian Mountains (Fig. 1). Plot location and measurements followed the technical recommendations for forest resource investigations described in Du et al. (2014). The plots were covered most of the spruce distribution on the north-facing slopes of the Qilian Mountains. Each plot was set 3 km along a transect from one other, but only if spruce forest was present and reachable. All plots were square with 28.28 m per side producing a sampled area of 0.08 ha. Plot location, number of trees, individual tree ages in five classes (young, middle, premature, mature, and old), mean tree diameter at breast height (i.e., 1.3 m; DBH), height (for trees with DBH > 5 cm), and tree density were recorded for each plot. According to the Technical Specifications on National Continuous Forest Inventory (Y.X. Zhang et al., 2020), the maximum allowable measurement error (tolerance) for DBH was 3 mm (for trees with a DBH lower than 20 cm) or 1.5 % (for trees with a DBH exceeding 20 cm). And tree height was measured using a traditional clinometer or an ultrasonic hypsometer, the tolerance for tree height measurement was 3 % (for trees <10 m) or 5 % (for trees over 10 m) (Zeng et al., 2015). Tree ages were classified according to the categories in Table S1.

### 2.3. Climate data

Annual mean precipitation (MAP) and annual mean temperature (MAT) from Climatic Research Unit gridded Time Series (CRU TS) 4.06 on 0.5° × 0.5° grids during 1981–2016 were used to analysis the relationship between spruce carbon density and climate factors (Harris et al., 2020). According to the climatic records, both MAP and MAT decrease from southeast to northwest of the Qilian Mountains (Fig. 2a, b), resulting in relatively wet conditions in southeast and relatively dry conditions in northwest. Specifically, MAP in the central Qilian Mountains was 250–350 mm, which was lower than in the eastern Qilian Mountains, where the precipitation reached 350–400 mm. Similarly, the MAT in the central Qilian Mountains ranged from −5 to −2 °C, which was colder than in the eastern Qilian Mountains, where the temperature ranged from 0 to 6 °C. Both the temperature and precipitation were increased during 1981–2016 (Fig. 2c, d), with the temperature increased 0.8 °C and the precipitation increased 35.7 mm during this period.

## 2.4. Data analysis and statistics

Biomass is the total dry weight of the organic matter of standing trees, including aboveground biomass and belowground biomass. Aboveground biomass includes the trunk (peeled), bark, branches (including fruits), and leaves (including flowers). Belowground biomass includes rhizomes, coarse roots (diameter > 10 mm), and fine roots (2 mm ≤ diameter ≤ 10 mm). Fibrous roots < 2 mm in diameter are not counted as root biomass. Instead, they are included as a portion of soil organic matter. We estimated the aboveground biomass (MA) and belowground biomass (MB) for the spruce according to the standard of Tree Biomass Models and Related Parameters to Carbon Accounting for *Picea* (LY/T 2655-2016) released from the China Forestry Administration (Zeng et al., 2016):

$$MA = 0.12890 DBH^{2.09828} H^{0.25663} (DBH \geq 5 \text{ cm})$$

$$MB = 0.056183 DBH^{2.54672} H^{-0.34753} (DBH \geq 5 \text{ cm})$$

Biomass and carbon densities of the trunks, bark, branches, and leaves of the trees were calculated according to the Biomass Models and Related Parameters to Carbon Accounting for *Picea* (Zeng et al., 2016). Carbon density was calculated as the product of biomass and the provided carbon-content coefficients according to the standard (Table S2). Here, carbon storage is the product of the carbon density and the spruce forest area. We estimated the mean biomass and carbon density for the different spruce age groups using all data sets from each of the three phases of the inventory. To analyze the spatial distribution of spruce biomass and carbon density, we further divided the study area into two regions according to mean annual precipitation: (i) the central Qilian Mountains (including the Heihe River basin) and (ii) the eastern Qilian Mountains (including Shiyang and Datong river basins) (Fig. 1). Biomass and carbon densities for each region were calculated following the same approach described above. Analysis of variance (ANOVA) and LSD's tests were used to test the statistical significance of differences in mean biomass and carbon density among age groups and regional groups.

To analyze the effects of topography, soil, understory vegetation, and stand characteristics on the carbon density of spruce, we calculated the Pearson correlation coefficients between the spruce carbon density and spatial topography characteristics (slope gradient), soil factors (soil depth and humus thickness), undergrowth properties (mean shrub

coverage and mean herb coverage), and age group. We also calculated the Pearson correlation between the mean value of carbon density of the three periods in each plot and corresponding MAT and MAP during 1981–2016 to evaluate the relationship between carbon density and climatic factors. The carbon density changes between 2006 and 2016 in each plot and related to climate factors during 2007–2016 were also calculated. To investigate the individual contribution of each environmental factor on mean carbon density and to changes in carbon density, we built linear mixed-effects models taking carbon density and changes carbon density as a function of climatic (MAT and MAP), stand age, soil (soil depth and humus thickness), and undergrowth factors (mean shrub coverage and mean herb coverage); carbon density and changes carbon density were the response variables in this analysis. Topography (slope direction and gradient) and subregion were included as random terms in the model. We avoided including interaction between fixed factors due to potentially high collinearity. Using variance inflation factors (VIFs) analyses as a guide, only VIFs < 5 was retained in the final model. For each model, marginal and conditional  $R^2$  values were calculated. The contribution of each independent variable was also calculated using a variance partitioning approach (Nakagawa and Schielzeth, 2013). Linear mixed-effects models were fitted using the R-package “lme4” (Bates et al., 2015).

## 3. Results

### 3.1. Biomass and carbon density

Most Qinghai spruce were middle-aged and in premature forest (Table S1), and most were distributed on north-facing slopes at 2600–3200 m asl (Fig. S1). Importantly, we found that both biomass and carbon density increased for spruce from 2006 to 2016. The mean biomasses were 133.80, 144.89, and 157.01 Mg ha<sup>-1</sup> in 2006, 2011, and 2016, respectively (Fig. 3a). Similarly, the mean biomass carbon densities were 65.52, 70.92, and 76.88 Mg C ha<sup>-1</sup> in 2006, 2011, and 2016, respectively (Fig. 3b). Over the decade of the survey period, mean biomass increased by 23.21 Mg ha<sup>-1</sup> (Fig. 4a), and the mean carbon density increased by 11.36 Mg C ha<sup>-1</sup> (Fig. 4b), corresponding to a 17.34 % increase from 2006 to 2016.

Aboveground, belowground, trunk, bark, branch, and leaf biomass increased by 17.09, 6.11, 8.70, 1.31, 4.75, and 2.34 Mg ha<sup>-1</sup> from 2006

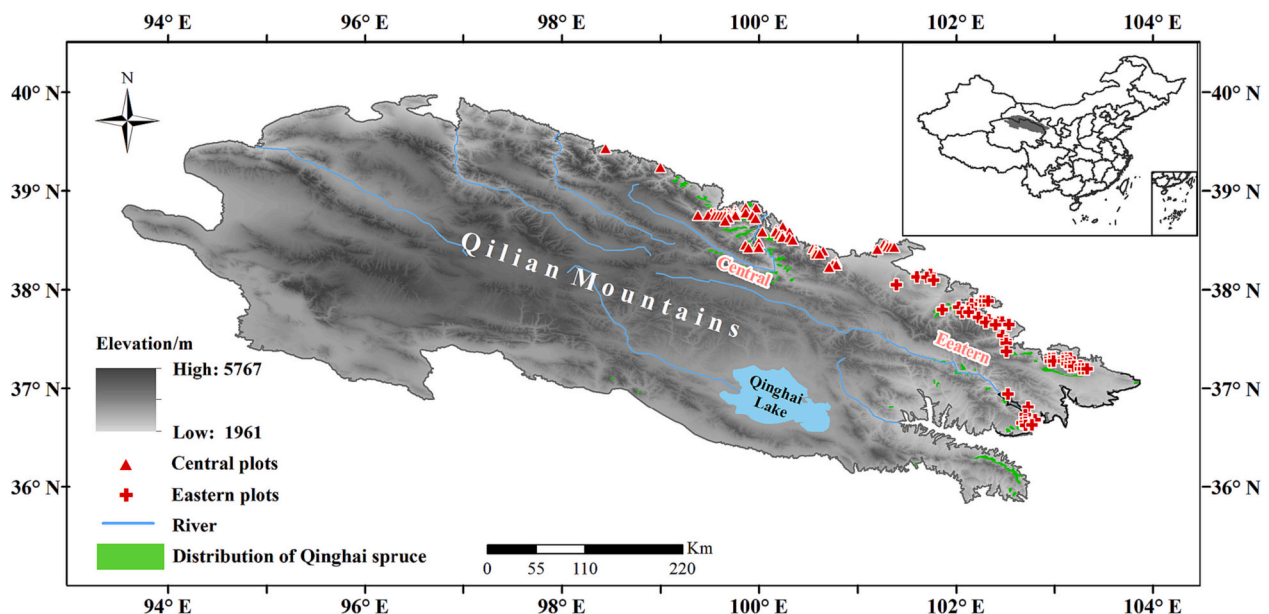
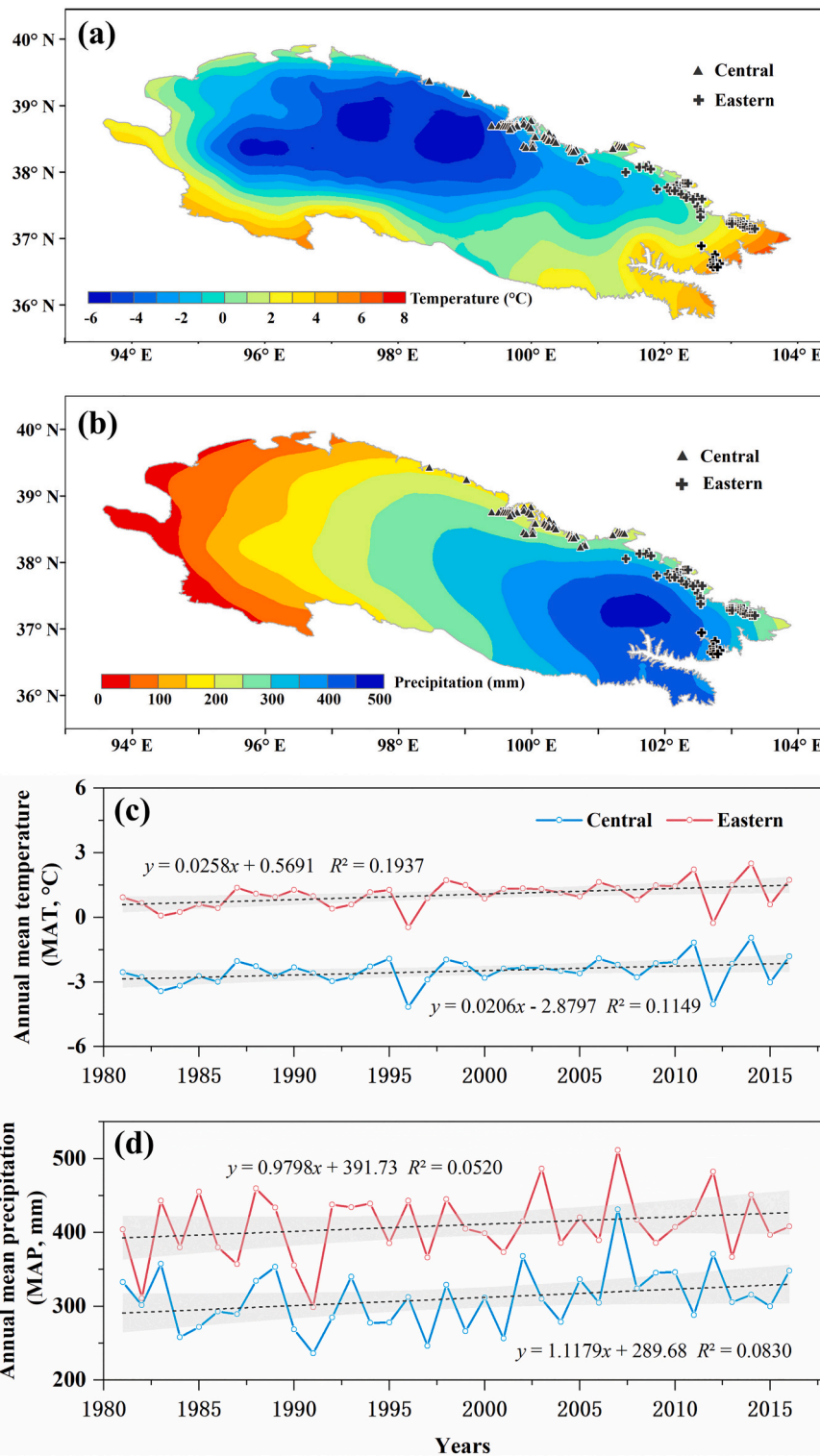


Fig. 1. Locations of the 104 study plots. The plots cover all distributions of spruce on the north-slope of the Qilian Mountains.

to 2016, respectively (Fig. 4a), while carbon densities increased by 8.38, 2.98, 4.22, 0.64, 2.35, and 1.17 Mg C ha<sup>-1</sup> from 2006 to 2016 for each portion of the ecosystem respectively (Fig. 4b). Mean carbon densities of young, middle, premature, mature, and old spruce forest were 10.03, 69.54, 72.18, 75.93, and 84.25 Mg C ha<sup>-1</sup>, respectively. Carbon density of the young group was found to be significantly lower than that of the

middle, premature, mature, and old groups ( $p < 0.05$ ). Carbon density of the middle group was found to be significantly lower than that of the old groups ( $p < 0.05$ ). There was no significant difference in the changes of carbon density among premature, mature, and old groups ( $p > 0.05$ ) (Fig. 5).



**Fig. 2.** Spatial distribution of the mean annual temperature (MAT) (a) and mean annual precipitation (MAP) (b), and interannual variation of MAT (c) and MAP (d) from CRU TS 4.06 during 1981–2016 of the Qilian Mountains. Symbols in (a) and (b) represent the sampling sites.

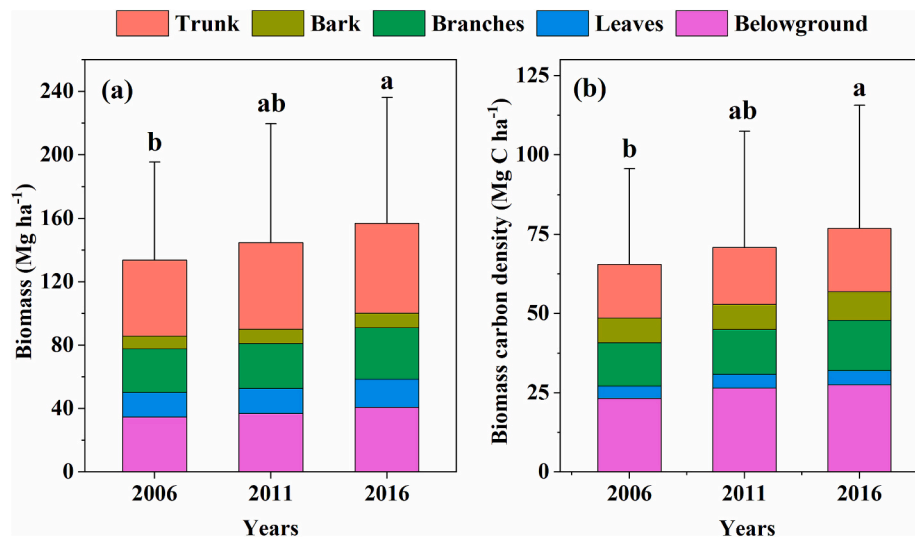


**Fig. 3.** (a) Biomass and (b) carbon density for different tree components in the three inventory years on the north-slope of the Qilian Mountains. The error bars indicate mean  $\pm$  one standard deviation (SD). Values bearing the same letters above bars are not significantly different at the 0.05 probability level (LSD test).

### 3.2. Total biomass and carbon storage

Total biomass for spruce in 2006, 2011, and 2016 were  $1.90 \times 10^7$ ,  $2.06 \times 10^7$ , and  $2.23 \times 10^7$  Mg, respectively, for a total increase of  $0.33 \times 10^7$  Mg in biomass over the inventory period (Table 1). Similarly, the amount of carbon stored in spruce in 2006, 2011, and 2016 were  $0.93 \times 10^7$ ,  $1.01 \times 10^7$ , and  $1.09 \times 10^7$  Mg C, respectively (Table 1) and results in an increase of carbon storage by  $0.16 \times 10^7$  Mg C.

### 3.3. Environmental forcing of carbon density

We found that age group was significantly correlated with carbon density both aboveground and belowground for spruce (Fig. S2). However, there was a significant negative correlation between the changes in carbon density and the stand age. There were significant negative correlations between carbon density and understory shrub and herb coverage due to competition between trees and understory vegetation.

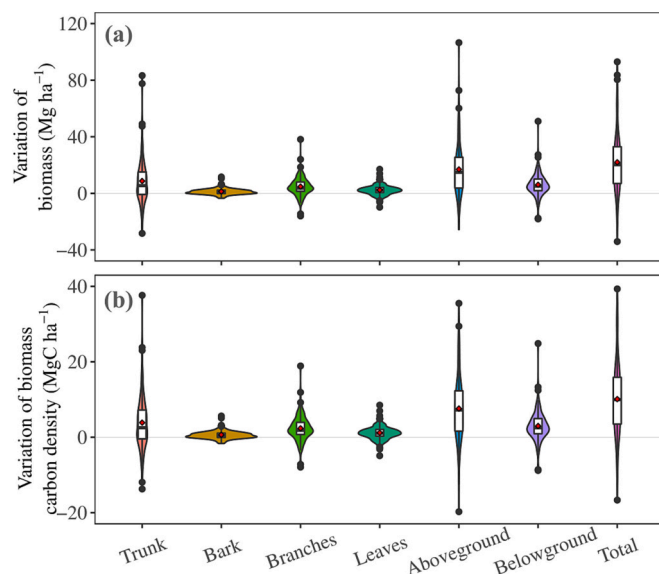


**Fig. 4.** Biomass and carbon density changes for different parts of spruce from 2006 to 2016. The rectangle in the middle of each density curve shows the ends of the first and third quartiles, and central red dot represents the median.

However, no significant relationship was found between understory vegetation and changes in the carbon density for spruce. Soil factors significantly affected the distribution of carbon density for spruce, and the changes of carbon density were also negatively correlated with slope gradient.

We found that total carbon density of trunk and bark was significantly positively correlated with MAT during 1981–2016 (Fig. 6a), and that changes in carbon density were significantly positively correlated both with MAP and MAT during 2007–2016 (Fig. 6b). However, no significant relationships were found between these climate factors and the belowground carbon density and their changes, indicating that climate factors mainly affected the growth of aboveground parts of the spruce, such as the trunk and bark. Linear mixed-effects modeling estimates suggests that both mean annual temperature and mean annual precipitation had significant effects on aboveground biomass carbon density (Table S3), contributing 21.8 % and 15.6 % to the variation in trunk carbon density, and 17.5 % and 11.7 % to the variation in bark density (Fig. 7a), respectively. Tree age and mean shrub coverage also had significant effects on carbon density (Table S3). Although fixed factors explained less variation in the changes in carbon density (Fig. 7b), mean annual temperature, age, and mean shrub coverage still had significant effects on changes in aboveground carbon density (Table S4).

### 3.4. Carbon density for different regions of the Qilian Mountains

To explore spatial patterns of spruce carbon density, we calculated carbon density of populations in the central and eastern portions of the Qilian Mountains, respectively, in the years 2006, 2011, and 2016. No significant differences in tree carbon density were found between the central and eastern populations in any of the studied years ( $p > 0.05$ ) (Fig. 8a). We found carbon densities increased in both regions to 8.41 and 14.43 Mg C ha<sup>-1</sup>, respectively, between 2006 and 2016. Carbon density increased by 21.5 % in the eastern and 13.2 % in the central Qilian Mountains during the study period, although no significant difference was found between the two regions ( $p = 0.054$ ) (Fig. 8b).

## 4. Discussion

### 4.1. Increasing forest carbon sinks in the Qilian Mountains

In this study, we found that the carbon density of the spruce forest increased by 11.36 Mg C ha<sup>-1</sup>, corresponding an increase of 17.34 % and

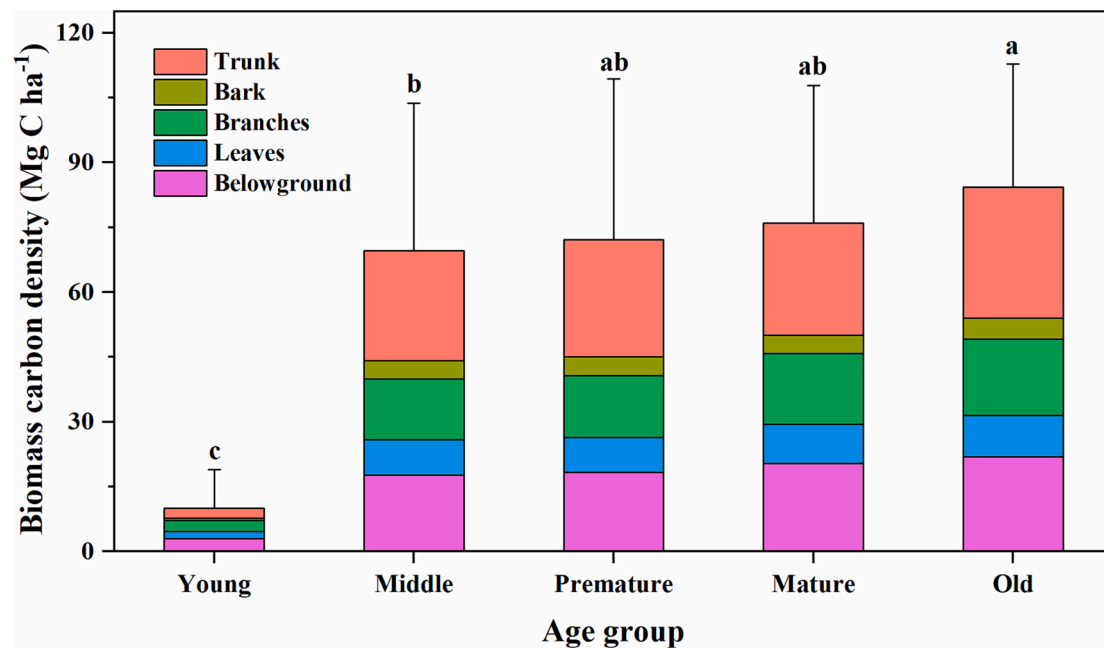


**Fig. 5.** Carbon densities for different ages of spruce. The aboveground carbon density is the sum of the carbon densities of the trunk, bark, branches, and leaves. The error bars indicate the mean  $\pm$  one standard deviation (SD) of the total carbon density. Values bearing the same letters above bars are not significantly different at the 0.05 probability level (LSD test).

**Table 1**

Total biomass, carbon storage, and carbon sequestration of spruce from 2006 to 2016 in the Qilian Mountains. Different lowercase letters within the same column indicate significant difference at the 0.05 level.

	Total biomass ( $\times 10^7$ Mg)	Carbon storage ( $\times 10^7$ Mg C)	Sequestration (Mg C ha <sup>-1</sup> yr <sup>-1</sup> )
2006	1.90 $\pm$ 0.88b	0.93 $\pm$ 0.43b	-
2011	2.06 $\pm$ 1.06ab	1.01 $\pm$ 0.52ab	1.08 $\pm$ 0.32a
2016	2.23 $\pm$ 1.13a	1.09 $\pm$ 0.55a	1.19 $\pm$ 0.33a

1.14 Mg C ha<sup>-1</sup> yr<sup>-1</sup> from 2006 to 2016 over the cold and arid Qilian Mountains. We found comparatively lower values reported in the literature in cold and arid areas relatively close to our region. [Chen et al. \(2018\)](#) reported carbon sequestration rates in spruce forest of 0.34 Mg C ha<sup>-1</sup> yr<sup>-1</sup> in trees in the Qinghai Province. In Tibetan Plateau broad-leaved forests, the average carbon sequestration rate was reported as 0.19 Mg C ha<sup>-1</sup> yr<sup>-1</sup> ([Wang et al., 2016](#)). Both sets of rates are lower than what we found in Spruce forests in the Qilian Mountains. Meanwhile, the carbon sequestration in subtropical and temperate forests of the central Himalaya varied from 3.99 to 4.83 Mg C ha<sup>-1</sup> yr<sup>-1</sup>, indicating that the rate of carbon sequestration for spruce in this study was lower than subtropical and temperate forests in the central Himalaya ([Joshi et al., 2021](#)). However, the rate of aboveground carbon

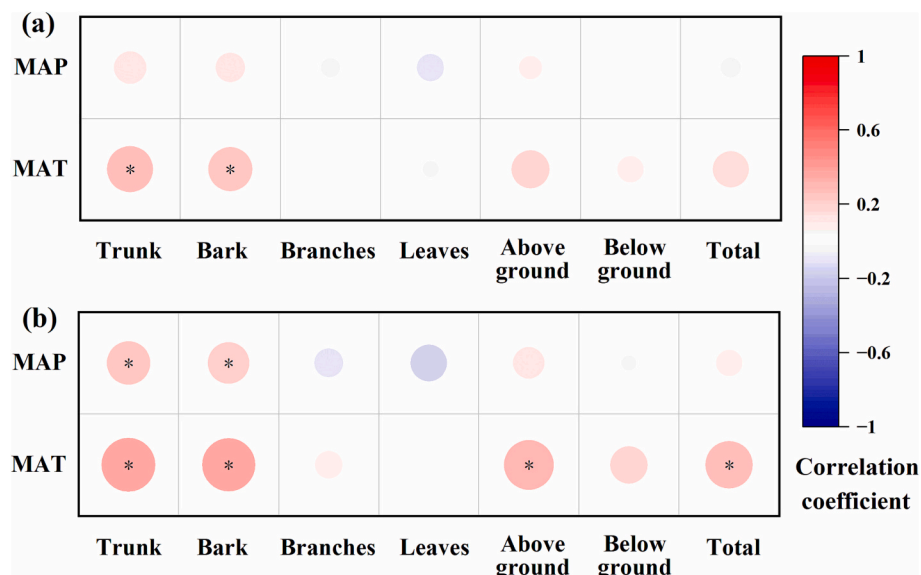


**Fig. 6.** Relationships between climate factors and (a) carbon density and (b) changes in carbon density from 2006 to 2016. For (a), annual mean precipitation (MAP), mean temperature (MAT) are the average values from 1981 to 2016; For (b), MAP and MAT are the average values from 2007 to 2016.

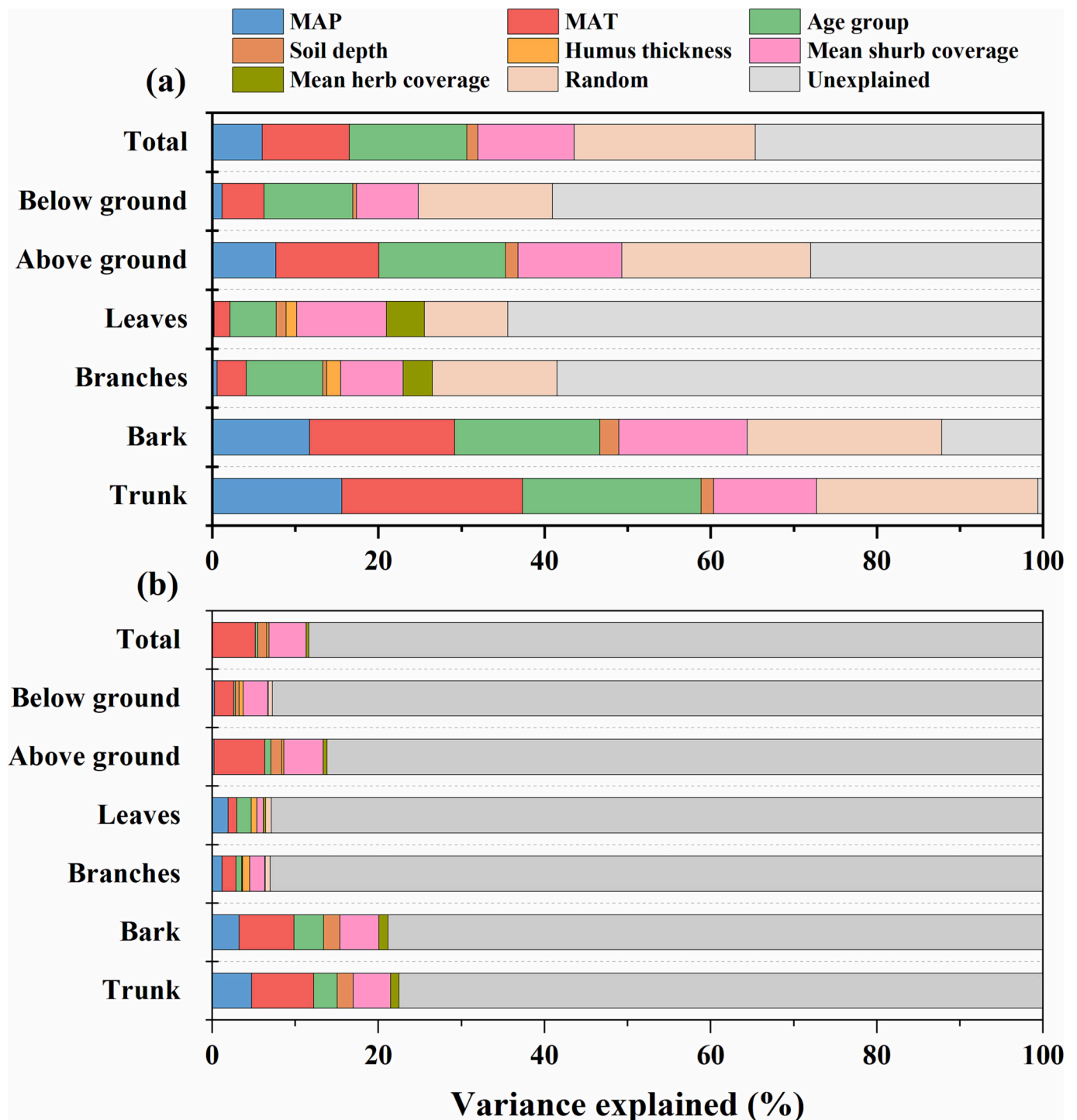


Fig. 7. Variance partition of the studied variables for (a) carbon density and (b) changes in carbon density from 2006 to 2016. Fixed variables include MAP, MAT, age group, soil depth, humus thickness, mean shrub and herb coverage. Random variables include slope direction, slope gradient, and subregions.

sequestration in the Qilian Mountains ( $0.84 \text{ Mg C ha}^{-1} \text{ yr}^{-1}$ ) was higher than the spruce forest in Tibetan of China (below  $0.5 \text{ Mg C ha}^{-1} \text{ yr}^{-1}$ ) (Sun et al., 2016). Additionally, the rate of forest carbon sequestration in China was  $0.41\text{--}1.19 \text{ Mg C ha}^{-1} \text{ yr}^{-1}$  (Chen et al., 2019) and the average carbon sequestration rate of national forest parks in China reached  $0.45 \text{ Mg C ha}^{-1} \text{ yr}^{-1}$  (Li et al., 2021). At the same period, the global forest biomass carbon sequestration capacity was  $-0.18\text{--}0.13 \text{ Mg C ha}^{-1} \text{ yr}^{-1}$  (Pan et al., 2011; FAO, 2020). Therefore, the results seem to reject our hypothesis that spruce carbon density and storage is much lower compared with the mean levels of national forest parks in China and

other regions. On the contrary, we found an increasing forest carbon sink for the cold and arid Qilian Mountains, rising at a higher rate than expected, despite the relative harsh growth in which these populations grow.

Due to the change in the total forested area of the Qilian Mountain was very small during the study period, the increase in the spruce carbon sink was mainly caused by the increase in the forest biomass carbon density. In this study, we calculated that the total spruce biomass carbon storage in the Qilian Mountains was  $10.93 \text{ Tg C}$  ( $1 \text{ Tg} = 10 \times 10^{12} \text{ g}$ ). For the same period, the mean biomass carbon that was stored in Gansu

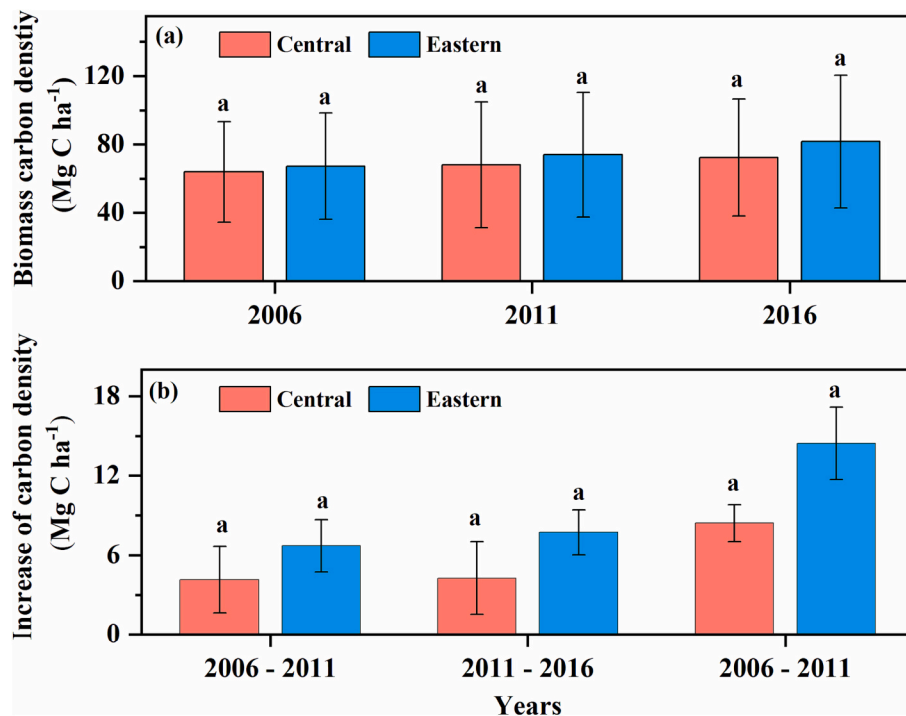


Fig. 8. Total mean carbon density (a) and increase in carbon density (b) between 2006 and 2016 across in regions in the Qilian Mountains. Values bearing the same letters above bars are not significantly different at the 0.05 probability level.

province and China was 98.84 and 8048 Tg C, respectively (Lin and Ge, 2019; FAO, 2020), suggesting that the spruce biomass carbon storage in the Qilian Mountains accounts for 11.06 % and 0.14 % of the total forest carbon storage in Gansu Province and China, respectively. Both carbon density and carbon storage for spruce have increased significantly in the Qilian Mountains, making an important contribution to carbon peaking and carbon neutrality of China.

#### 4.2. Environmental and climatic forcings for carbon density

We found no significant relationship between vegetation and changes in spruce carbon density, which suggests that it is not necessary to remove vegetation from the forest to improve the forest carbon density. This result indicated that the integrity of forest structure can therefore be preserved while also increasing carbon density. Carbon density was significantly positively correlated with stand density and canopy density, indicating that stand mass has been the main driver for carbon density increases in recent years in our study region. There was a significant negative correlation between the changes in carbon density and the stand age, indicating that carbon sequestration capacity decreases as age increases. Soil factors significantly affected the distribution of, and changes in, the carbon density for spruce expect the changes of carbon density in branches and leaves, since deeper soil and humus provide more soil nutrients and water, which are benefitted for spruce growth. Increases in carbon density were significantly negatively impacted by slope, mainly because a high slope gradient weakens the soil water retention capacity due to altitude and thus affects spruce growth. There were also no significant disturbances in our forests during this period, so the trends found here might represent a kind of maximum potential. Young stands tend to have strong carbon sequestration capacity, while forests at the old age group store more carbon and can sequester it continuously (Mildrexler et al., 2020; Jiang et al., 2020; Stephenson et al., 2014).

The Qilian Mountains cover a wide range of altitudes, latitudes, and longitudes, creating large spatial differences in temperature and

precipitation, which result in large regional differences for spruce biomass and carbon density. In this study, both the correlation and linear mixed-effects model showed that MAP was positively correlated with changes of carbon density in aboveground carbon pools, such as the trunk and bark, whereas there was no significant relationship between carbon density and changes in the belowground carbon pools. These findings suggest that precipitation may have the strongest effect on radial tree growth and little impact on belowground root growth. Many tree-ring studies have shown that precipitation is the main factor that affects radial spruce growth in this region (Tian et al., 2017; Gao et al., 2018), but research on the climatic impacts on belowground accumulation in this region are unknown to us. Spruce has the largest distribution area and the widest range of all tree species in the Qilian Mountains; its growth depends mainly on water availability, especially in drought-restricted areas (Wang et al., 2020). Drought reduces the soil moisture and increases the influence of evapotranspiration on spruce carbon density in the arid Qilian Mountains (Wu et al., 2015). Additionally, MAT was also significantly correlated with the changes of carbon densities aboveground, indicating that temperature also play an important role on the increase of carbon density aboveground. Warm temperatures may extend growing season of spruce, resulting in an increase in tree growth in the Qilian Mountains. Gao et al. (2018) found that the number of days per year with a daily mean temperature higher than 5 °C has increased by about 10 days during the past six decades over the Qilian Mountains. Yang et al. (2017) found that the onset of the growing season has been advanced, and the end of the growing season has been delayed of Qilian juniper across the Tibetan Plateau over the period 1960–2014, changes that mirror regional climate changes. Several studies have shown that the lengthening of the growing season will accelerate tree growth in Qilian Mountains (Zhang et al., 2021), and high latitude and high elevation forests (Rossi et al., 2016; Huang et al., 2020). Therefore, we conclude that the changes in above-ground carbon density over the past decade may have been influenced by an interaction of precipitation and temperature.

#### 4.3. Effects of age on carbon density

Forests continue to accumulate carbon as their age increasing (Eileen et al., 2001; Bradford and Kastendick, 2010; Besnard et al., 2018), although their growth efficiency appears to decrease (Keith et al., 2009; Lewis et al., 2009; Sillett et al., 2015; Musavi et al., 2017). The rate of carbon sequestration and carbon storage for a forest cannot reach a maximum at the same time (Kurz et al., 2013). Young stands tend to have strong carbon sequestration capacity, while forests in the older age groups store large amounts of carbon. Our findings for the carbon density for spruce forest support these general trends. We found that carbon density increased with forest age, but that the carbon sequestration rate decreased with increasing forest age. There remains much debate over whether old forests are carbon sinks, but we found that the carbon density for the mature and old spruce forests in our study are still increasing. Our study suggests that it is not appropriate to categorize spruce forest that is older than 140 years as unproductive. Others have found that a forest may cease to be a carbon sink when they are as old as 450–500 years (Liu et al., 2014). The average age of spruce forests in the Qilian Mountains is <100 years while most forests are middle-age and near-mature forests (Table S1). Average tree age in these forests seems to influence the rate of carbon sequestration for spruce in the Qilian Mountains. Similarly, young forests have higher photosynthetic capacity and carbon sequestration rate likely contribute to the difference in trend and estimate between our target study and previous work (Musavi et al., 2017; Zhang et al., 2023). Indeed, a study on the edge of the Negev Desert found relatively higher carbon sequestration rates (1–2 Mg C ha<sup>-1</sup> yr<sup>-1</sup>) in 35-year-old dry forests (Grünzweig et al., 2003). Despite the recognized effects of forest age in controlling forest carbon balance, there is still debate about the quantitative role of forest age in the empirical annual forest carbon estimates (Besnard et al., 2018). In our analysis, the rate of carbon density seems to be increasing with tree age. While that matches what others have found elsewhere (Pan et al., 2004; Bradford and Kastendick, 2010), there is much more to investigate on drivers on the rate of carbon density over time.

#### 4.4. Carbon density spatial variability

We found no significant difference in carbon density for spruce between the central and eastern in Qilian Mountains. The change in carbon density was higher for the eastern Qilian Mountains than central region, which means that the spruce growth rate in the eastern Qilian Mountains is higher than that in the central region due to the influences of the stand ages and the climate. In future, the carbon sequestration potential for the eastern Qilian Mountains will therefore be greater than for other regions of the Qilian Mountains, though a lot of this depends on the future disturbance and climate dynamics.

There are several possible explanations for our geographic results. The spruce forests in the eastern Qilian Mountains are younger, and therefore have a higher growth rate than the spruce forests in central region (J.Z. Zhang et al., 2020). Also, spruce growth is significantly affected by precipitation and temperature (Tian et al., 2017; Gao et al., 2018; Wang et al., 2020) and both the temperature and precipitation are significantly higher in the eastern Qilian Mountains than in the central (Xu et al., 2013; Qiang et al., 2016).

#### 4.5. Caveats and a larger context for our study

The carbon that accumulates in the forest through CO<sub>2</sub> absorption via photosynthesis is mainly stored in the aboveground biomass, belowground biomass, soil organic carbon, dead wood, and in the litter (FAO, 2020). Deforestation causes some of the accumulated carbon to leave the forest ecosystem in the form of timber products. However, ecological forest projects such as Natural Forest Protection Project, have led to deforestation being banned in the Qilian Mountains since 1998 (Zhang et al., 2000). Therefore, in our study, we did not consider any

changes in carbon that were due to deforestation and focused mainly on the carbon pool stored in the aboveground and belowground biomass. The aboveground biomass carbon pools were considered separately for the trunk, bark, branches, and leaves. We did not investigate the carbon stored in the understory vegetation, surface drops, and soil, and so the biomass carbon storage that we calculated includes only the carbon stored in standing trees and may not reflect the full extent of the forest ecosystem carbon sink.

Many factors can lead to uncertainty in estimating forest carbon sinks (Pan et al., 2011; Sun et al., 2016). Samples with good growth are often preferentially selected in studies that use forest sample plots due to the subjective choices made by humans, and this can lead to inappropriately high estimates of biomass and carbon density (Fang et al., 1998). In our study, we used the same selection criteria for all survey areas, and calculated a large forest inventory that offers improved accuracy over existing estimates of carbon stock changes (Li et al., 2012). The different biomass conversion coefficients that are used for different forest age groups can also lead to differences in carbon sink estimates (Pan et al., 2004). More assessments and further comparative studies are needed to improve existing estimates and reduce their uncertainty.

## 5. Conclusions

In this study, we carried out a three-phase forest inventory for 104 permanent sample plots that cover all areas of the spruce forest distribution in the Qilian Mountains, calculating the inventory every five years from 2006 to 2016. These forest inventories allowed us to accurately estimate spruce forest biomass-carbon density at regional scales and to improve predictions of the likely effects of climate change. We found that spruce carbon density increased by 17.34 % from 2006 to 2016 over the Qilian Mountains. Both the precipitation and temperature play important roles on the increase of aboveground carbon density. Mature and old trees fixed the most carbon during the period of study. The most dramatic difference in fixed carbon occurred nearly the first four decades of spruce growth. According to our assessment, the carbon sequestration rate for spruce in the cold and arid Qilian Mountains is significantly higher than the average rates of the national forest parks in China, despite the relatively severe growth environment.

### CRedit authorship contribution statement

Xiaohua Gou and Junzhou Zhang designed the project. Zongying Cao and Junzhou Zhang verified the analytical methods and wrote the manuscript. Yuetong Wang, Qipeng Sun and Jiqin Yang provided data collation and part of the mapping work. Xiaohua Gou, Rubén D. Manzanedo and Neil Pederson contributed to the interpretation of the results and supervised the findings of this work. All authors discussed the results and contributed to the final manuscript.

### Declaration of competing interest

The authors declare that they have no known competing financial interests or personal relationships that could have influenced the work reported in this paper.

### Data availability

Data is available on request by contact with the corresponding authors.

### Acknowledgments

The authors are grateful to Gansu Qilian Mountains National Nature Reserve and Gansu Ecological Resources Monitoring Center for supporting this article. Special thanks to Xuhua Zhang and Zhiping Liu for their support of the investigation norms and policy documents. This

work was supported by the Second Tibetan Plateau Scientific Expedition and Research Program (STEP; No.2019QZKK0301), and the National Natural Science Foundation of China (No. U21A2006 and 42001043).

## Appendix A. Supplementary data

Supplementary data to this article can be found online at <https://doi.org/10.1016/j.scitotenv.2023.167168>.

## References

- Abdelhak, M., 2022. Natural Resources Conservation and Advances for Sustainability. Section A: Natural resources management. Chapter 4: Soil improvement in arid and semiarid regions for sustainable development. Copyright © 2022 Elsevier Inc., pp. 73–90.
- Bates, D.M., Mächler, M., Bolker, B.M., Walker, S., 2015. lme4: linear mixed-effects models using Eigen and S4. R package version 1.1-8. <http://CRAN.R-project.org/package=lme4>.
- Besnard, S., Carvalhais, N., Arain, M.A., Black, A., de Bruin, S., Buchmann, N., Cescatti, A., Chen, J., Clevers, J.G.P.W., Desai, A.R., Gough, C.M., Havrankova, K., Herold, M., Hörtnagl, L., Jung, M., Knohl, A., Kruijt, B., Krupkova, L., Law, B.E., Lindroth, A., Noormets, A., Rouspard, O., Steinbrecher, R., Varlagin, A., Vincke, C., Reichstein, M., 2018. Quantifying the effect of forest age in annual net forest carbon balance. *Environ. Res. Lett.* 13 (12), 124018. <https://doi.org/10.1088/1748-9326/aaeab>.
- Bradford, J.B., Kastendick, D.N., 2010. Age-related patterns of forest complexity and carbon storage in pine and aspen-birch ecosystems of northern Minnesota, USA. *Can. J. For. Res.* 40, 401–409. <https://doi.org/10.1139/X10-002>.
- Chang, X.X., Zhao, W.Z., Liu, H., Wei, X., Liu, B., He, Z.B., 2014. Qinghai spruce (*Picea crassifolia*) forest transpiration and canopy conductance in the upper Heihe River Basin of arid northwestern China. *Agric. For. Meteorol.* 198–199, 209–220. <https://doi.org/10.1016/j.agrformet.2014.08.015>.
- Chen, K.Y., Zi, H.B., Adeluji, Hu, L., Wang, G.X., Wang, C.T., 2018. Current stocks and potential of carbon sequestration of the forest tree layer in Qinghai Province, China. *Chinese J. Plant Ecol.* 42 (8), 831–840. <https://doi.org/10.17521/cjpe.2018.0058>.
- Chen, A.P., Peng, S.S., Fei, S.L., 2019. Mapping global forest biomass and its changes over the first decade of the 21st century. *Sci. China Earth Sci.* 62, 585–594. <https://doi.org/10.1007/s11430-018-9277-6>.
- Du, L., Zhou, T., Zou, Z.H., Zhao, X., Huang, K.C., Wu, H., 2014. Mapping forest biomass using remote sensing and national forest inventory in China. *Forests* 5 (6), 1267–1283. <https://doi.org/10.3390/f5061267>.
- Eileen, V.C., Anna, S., Robert, K., Ragan, M.C., 2001. Are old forests underestimated as global carbon sinks? *Glob. Chang. Biol.* 7, 339–344. <https://doi.org/10.1046/j.1365-2486.2001.00418.xc>.
- Fang, J.Y., Wang, G.G., Liu, G.H., Xu, S.L., 1998. Forest biomass of China: an estimate based on the biomass–volume relationship. *Ecol. Appl.* 8 (4), 1084–1091. [https://doi.org/10.1890/1051-0761\(1998\)008\[1084:FBOCAE\]2.0.CO;2](https://doi.org/10.1890/1051-0761(1998)008[1084:FBOCAE]2.0.CO;2).
- Fang, J.Y., Guo, Z.D., Hu, H.F., Kato, T., Muraoka, H., Son, Y.W., 2014. Forest biomass carbon sinks in East Asia, with special reference to the relative contributions of forest expansion and forest growth. *Glob. Chang. Biol.* 20 (6), 2019–2030. <https://doi.org/10.1111/gcb.12512>.
- Fang, J.Y., Yu, G.R., Liu, L.L., Hu, S.J., Chapin, F.S., 2018. Climate change, human impacts, and carbon sequestration in China. *Proc. Natl. Acad. Sci. U. S. A.* 115 (16), 4015–4020. <https://doi.org/10.1073/pnas.1700304115>.
- FAO, 2020. Global Forest Resources Assessment 2020. Food and Agriculture Organization of the United Nations. <https://fra-data.fao.org/WO/fra2020/home/>.
- Friedlingstein, P., O'Sullivan, M., Jones, M.W., Andrew, R.M., Hauck, J., Olsen, A., Peters, G.P., Peters, W., Pongratz, J., Sitch, S., Le Quéré, C., Canadell, J.G., Ciais, P., Jackson, R.B., Alin, S., Aragão, L.E.O.C., Arneeth, A., Arora, V., Bates, N.R., Zaehle, S., 2020. Global Carbon Budget 2020. *Earth Syst. Sci. Data* 12, 3269–3340. <https://doi.org/10.5194/essd-12-3269-2020>.
- Fu, J.X., Cao, G.C., Guo, W.J., 2020. Changes of growing season NDVI at different elevations, slopes, slope aspects and its relationship with meteorological factors in the southern slope of the Qilian Mountains, China from 1998 to 2017. *Chin. J. Appl. Ecol.* 31 (4), 1203–1212. <https://doi.org/10.13287/j.1001-9332.202004.018>.
- Gao, L.L., Gou, X.H., Deng, Y., Wang, Z.Q., Wang, F., 2018. Increased growth of Qinghai spruce in northwestern China during the recent warming hiatus. *Agric. For. Meteorol.* 260–261, 9–16. <https://doi.org/10.1016/j.agrformet.2018.05.025>.
- Gibbs, H.K., Brown, S., Niles, J.O., Jonathan, A., Foley, J.A., 2007. Monitoring and estimating tropical forest carbon stocks: making REDD a reality. *Environ. Res. Lett.* 2, 1–13. <https://doi.org/10.1088/1748-9326/2/4/045023>.
- Gil, M.V., Blanco, D., Carballo, M.T., Calvo, L.F., 2011. Carbon stock estimates for forests in the Castilla y León region, Spain. A GIS based method for evaluating spatial distribution of residual biomass for bio-energy. *Biomass Bioenergy* 35 (1), 243–252. <https://doi.org/10.1016/j.biombioe.2010.08.004>.
- Gómez-García, E., 2020. Estimating the changes in tree carbon stocks in Galician forests (NW Spain) between 1972 and 2009. *Forest Ecol. Manag.* 467, 118157. <https://doi.org/10.1016/j.foreco.2020.118157>.
- Grünzweig, J.M., Lin, T., Rotenberg, E., Schwartz, A., Yakir, D., 2003. Carbon sequestration in arid-land forest. *Glob. Chang. Biol.* 9 (5), 791–799. <https://doi.org/10.1046/j.1365-2486.2003.00612.x>.
- Harris, I., Osborn, T.J., Jones, P., Lister, D., 2020. Version 4 of the CRU TS monthly high-resolution gridded multivariate climate dataset. *Sci. Data* 7, 109. <https://doi.org/10.1038/s41597-020-0453-3>.
- Houghton, R.A., 2005. Aboveground forest biomass and the global carbon balance. *Glob. Chang. Biol.* 11, 945–958. <https://doi.org/10.1111/j.1365-2486.2005.00955.x>.
- Houghton, R.A., 2020. Terrestrial fluxes of carbon in GCP carbon bud-gets. *Glob. Chang. Biol.* 26, 3006–3014. <https://doi.org/10.1111/gcb.15050>.
- Huang, J.G., Ma, Q.Q., Rossi, S., Biondi, F., Deslauriers, A., Fonti, P., Liang, E.Y., Mäkinen, H., Oberhuber, W., Cyrille, R., Tognetti, R., Tremli, V., Yang, B., Zhang, J. L., Antonucci, S., Bergeron, Y., Camarero, J.J., Campelo, F., Cufar, K., Ziaca, L.O., 2020. Photoperiod and temperature as dominant environmental drivers triggering secondary growth resumption in Northern Hemisphere conifers. *Proc. Natl. Acad. Sci. U.S.A.* 117 (34), 20645–20652. <https://doi.org/10.1073/pnas.2007058117>.
- Jiang, M.K., Medlyn, B.E., Drake, J.E., Duursma, R.A., Anderson, I.C., Ellsworth, D.S., 2020. The fate of carbon in a mature forest under carbon dioxide enrichment. *Nature* 580, 227–231. <https://doi.org/10.1101/696898>.
- Joshi, V.C., Negi, V.S., Bisht, D., Sundriyal, R.C., Arya, D., 2021. Tree biomass and carbon stock assessment of subtropical and temperate forests in the Central Himalaya, India. *Trees Forests People* 6, 100147. <https://doi.org/10.1016/j.tfp.2021.100147>.
- Keith, H., Mackey, B.G., Lindenmayer, D.B., 2009. Re-evaluation of forest biomass carbon stocks and lessons from the world's most carbon-dense forests. *Proc. Natl. Acad. Sci. U. S. A.* 106 (28), 11635–11640. <https://doi.org/10.1073/pnas.0901970106>.
- Kindermann, G.E., Mccallum, I., Fritz, S., Obersteiner, M., 2008. A global forest growing stock, biomass and carbon map based on FAO statistics. *Silva Fenn.* 42 (3), 387–396. <https://doi.org/10.14214/sf.244>.
- Kurz, W.A., Shaw, C.H., Boisvenue, C., Stinson, G., Metsaranta, J., Leckie, D., Dyk, A., Smyth, C., Neilson, E.T., 2013. Carbon in Canada's boreal forest – a synthesis. *Environ. Rev.* 21, 260–292. <https://doi.org/10.1139/er-2013-0041>.
- Le Noë, J., Matej, S., Magerl, A., Bhan, M., Erb, K.H., Gingrich, S., 2020. Modeling and empirical validation of long-term carbon sequestration in forests (France, 1850–2015). *Glob. Chang. Biol.* 26, 2421–2434. <https://doi.org/10.1111/gcb.15004>.
- Lewis, S.L., Lopez-Gonzalez, G., Sonké, B., Affum-Baffoe, K., Baker, T.R., Ojo, L.O., Phillips, O.L., Reitsma, J.M., White, L., Comiskey, J.A., Marie-Noël, D.K., Ewango, C. E.N., Feldpausch, T.R., Hamilton, A.C., Gloor, M., Hart, T., Hladik, A., Lloyd, J., Lovett, J.C., Makana, J.R., Malhi, Y., Mbago, F.M., Ndangalasi, H.J., Peacock, J., Peh, K.S.H., Sheil, D., Sunderland, T., Swaine, M.D., Taplin, J., Taylor, D., Thomas, S. C., Votere, R., Wöll, H., 2009. Increasing carbon storage in intact African tropical forests. *Nature* 457, 1003–1006. <https://doi.org/10.1038/nature07771>.
- Li, H.K., Zhao, P.X., Lei, Y.C., Zeng, W.S., 2012. Comparison on estimation of wood biomass using forest inventory data. *Sci. Silvae Sin.* 48 (5), 44–52. <https://doi.org/10.11707/j.1001-7488.20120507>.
- Li, W., Huang, M., Zhang, Y.D., Gu, F.X., Gong, H., Guo, R., Zhong, X.L., Yan, C.R., 2021. Spatial-temporal variations of carbon storage and carbon sequestration rate in China's national forest parks. *Chin. J. Appl. Ecol.* 32 (3), 799–809. <https://doi.org/10.13287/j.1001-9332.202103.015>.
- Lin, B.Q., Ge, J.M., 2019. Valued forest carbon sinks: how much emissions abatement costs can be reduced in China. *J. Clean. Prod.* 224, 455–464. <https://doi.org/10.1016/j.jclepro.2019.03.221>.
- Liu, Y.C., Yu, G.R., Wang, Q.F., Zhang, Y.J., 2014. How temperature, precipitation and stand age control the biomass carbon density of global mature forests. *Glob. Ecol. Biogeogr.* 23, 323–333. <https://doi.org/10.1111/gcb.12113>.
- Liu, F., Zhang, Q., Van, D.A.R., Zheng, B., Tong, D., Yan, L., Zheng, Y.X., He, K.B., 2016. Recent reduction in NOX emissions over China: synthesis of satellite observations and emission inventories. *Environ. Res. Lett.* 11 (11), 1–9. <https://doi.org/10.1088/1748-9326/11/11/114002>.
- Liu, Y.C., Gao, X.L., Fu, C., Yu, G.R., Liu, Z.Y., 2019. Estimation of carbon sequestration potential of forest biomass in China based on National Forest Resources Inventory. *Acta Ecol. Sin.* 39 (11), 4002–4010. <https://doi.org/10.5846/xbx201805701016>.
- Lu, F., Hu, H.F., Sun, W.J., Zhu, J.J., Liu, G.B., Zhou, W.M., Zhang, Q.F., Shi, P.L., Liu, X. P., Wu, X., Zhang, L., Wei, X.H., Dai, L.M., Zhang, K.R., Sun, Y.R., Xue, S., Zhang, W. J., Xiong, D.P., Deng, L., Liu, B.J., Zhou, L., Zhang, C., Zheng, C., Cao, J.S., Huang, Y., He, N.P., Zhou, G.Y., Bai, Y.F., Xie, Z.Q., Tang, Z.Y., Wu, B.F., Fang, J.Y., Liu, G.H., Yu, G.R., 2018. Effects of national ecological restoration projects on carbon sequestration in China from 2001 to 2010. *Proc. Natl. Acad. Sci. U. S. A.* 115 (16), 4039–4044. <https://doi.org/10.1073/pnas.1700294115>.
- Malagnoux, M., 2007. Arid land forests of the world: global environmental perspectives. <https://www.fao.org/3/ah836e/ah836e.pdf>.
- Mildredler, D.J., Berner, L.T., Law, B.E., Richard, A., Birdsey, R.A., Moomaw, W.R., 2020. Large trees dominate carbon storage in forests east of the Cascade Crest in the United States Pacific Northwest. *Front. For. Glob. Change* 3 (127), 59427. <https://doi.org/10.3389/ffgc.2020.59427>.
- Musavi, T., Migliavacca, M., Reichstein, M., Kattge, J., Wirth, C., Black, T.A., Janssens, I., Knohl, A., Loustau, D., Rouspard, O., Varlagin, A., Rambal, S., Cescatti, A., Gianeelle, D., Kondo, H., Tamrakar, R., Mahecha, M.D., 2017. Stand age and species richness dampen interannual variation of ecosystem-level photosynthetic capacity. *Nat. Ecol. Evol.* 1, 48. <https://doi.org/10.1038/s41559-016-0048>.
- Nabuurs, G.J., Schelhaas, M.J., Mohren, G.M.J., Field, C.B., 2003. Temporal evolution of the European forest sector carbon sink from 1950 to 1999. *Glob. Chang. Biol.* 9, 152–160. <https://doi.org/10.1046/j.1365-2486.2003.00570.x>.
- Nakagawa, S., Schielzeth, H., 2013. A general and simple method for obtaining  $R^2$  from generalized linear mixed-effects models. *Methods Ecol. Evol.* 4 (2), 133–142. <https://doi.org/10.1111/j.2041-210x.2012.00261.x>.
- O'Sullivan, M., Spracklen, D.V., Batterman, S.A., Arnold, S.R., Gloor, M., Buermann, W., 2019. Have synergies between nitrogen deposition and atmospheric CO<sub>2</sub> driven the

- recent enhancement of the terrestrial carbon sink? *Global Biogeochem. Cycles* 33, 163–180. <https://doi.org/10.1029/2018GB005922>.
- Pan, Y.D., Luo, T.X., Birdsey, R., Hom, J., Melillo, J., 2004. New estimates of carbon storage and sequestration in China's forests: effects of age-class and method on inventory-based carbon estimation. *Clim. Change* 67 (2–3), 211–236. <https://doi.org/10.1007/s10584-004-2799-5>.
- Pan, Y., Birdsey, R.A., Fang, J., Houghton, R., Kauppi, P.E., Kurz, W.A., Phillips, O.L., Shvidenko, A., Lewis, S.L., Canadell, J.G., Ciais, P., Jackson, R.B., Pacala, S.W., McGuire, A.D., Piao, S., Rautiainen, A., Sitch, S., Hayes, D., 2011. A large and persistent carbon sink in the world's forests. *Science* 333, 988–993. <https://doi.org/10.1126/science.1201609>.
- Piao, S.L., Fang, J.Y., Zhu, B., Tan, K., 2005. Forest biomass carbon stocks in China over the past 2 decades: estimation based on integrated inventory and satellite data. *J. Geophys. Res.* 110, G01006 <https://doi.org/10.1029/2005JG000014>.
- Piao, S.L., Fang, J.Y., Ciais, P., Peylin, P., Huang, Y., Sitch, S., Wang, T., 2009. The carbon balance of terrestrial ecosystems in China. *Nature* 458 (7241), 1009–1013. <https://doi.org/10.1038/nature07944>.
- Qian, D.W., Cao, G.M., Du, Y.G., Li, Q., Guo, X.W., 2020. Spatio-temporal dynamics of ecosystem service value in the southern slope of Qilian Mountain from 2000 to 2015. *Acta Ecol. Sin.* 40 (4), 1392–1404. <https://doi.org/10.5846/stxb201811292598>.
- Qiang, N., Zhang, M.J., Wang, S.J., Liu, Y.M., Ren, Z.G., Zhu, X.F., 2016. Estimation of areal precipitation in the Qilian Mountains based on a gridded dataset since 1961. *J. Geogr. Sci.* 26 (1), 59–69. <https://doi.org/10.1007/s11442-016-1254-7>.
- Rossi, S., Anfodillo, T., Cufar, K., Cuny, H.E., Deslauriers, A., Fonti, P., Frank, D., Gricar, J., Gruber, A., Huang, J.G., Jyske, T., Kaspar, J., King, G., Krause, C., Liang, E.Y., Mäkinen, H., Morin, H., Nöjd, P., Oberhuber, W., Prislán, P., Rathgeber, C.B.K., Saracino, A., Swidrak, I., Tremli, V., 2016. Pattern of xylem phenology in conifers of cold ecosystems at the Northern Hemisphere. *Glob. Chang. Biol.* 22 (11), 3804–3813. <https://doi.org/10.1111/gcb.13317>.
- Sillett, S.C., Pelt, R.V., Kramer, R.D., Carroll, A.L., Koch, G.W., 2015. Biomass and growth potential of *Eucalyptus regnans* up to 100 m tall. *Forest Ecol. Manag.* 348, 78–91. <https://doi.org/10.1016/j.foreco.2015.03.046>.
- Smith, P., Bustamante, M., Ahammad, H., Clark, H., Dong, H., Elsidig, E., Tubiello, F., 2014. Agriculture, forestry and other land use (AFOLU). In: Edenhofer, O., Pichs-Madruga, R., Sokona, Y., Farahani, E., Kadner, S., Seyboth, K., Adler, A., Baum, I., Brunner, S., Eickemeier, P., Kriemann, B., Savolainen, J., Schlömer, S., Stechow, C., Zwinkel, T., Minx, J. (Eds.), *Climate Change 2014: Mitigation of Climate Change. Contribution of Working Group III to the Fifth Assessment Report of the Intergovernmental Panel on Climate Change*. Cambridge University Press, Cambridge, UK and New York, NY, pp. 1–179.
- Stephenson, N.L., Das, A.J., Condit, R., Russo, S.E., Baker, P.J., Beckman, N.G., Coomes, D.A., Lines, E.R., Morris, W.K., Rüger, N., Álvarez, E., Blundo, C., Bunyavechewin, S., Chuyong, G., Davies, S.J., Duque, A., Ewango, C.N., Flores, O., Franklin, J.F., Grau, H.R., Hao, Z., Harmon, M.E., Hubbell, S.P., Kenfack, D., Lin, Y., Makana, J.R., Malizia, A., Malizia, L.R., Pabst, R.J., Pongpattananurak, N., Sun, S.H., Sun, I.F., Tan, S., Thomas, D., van Mantgem, P.J., Wang, X., Wisser, S.K., Zavala, M. A., 2014. Rate of tree carbon accumulation increases continuously with tree size. *Nature* 507, 90–93. <https://doi.org/10.1038/nature12914>.
- Sun, X.Y., Wang, G.X., Huang, M., Chang, R.Y., Ran, F., 2016. Forest biomass carbon stocks and variation in Tibet's carbon-dense forests from 2001 to 2050. *Sci. Rep.* 6 (1), 19–27. <https://doi.org/10.1038/srep34687>.
- Tian, X., Yan, M., Christiaan, V.T., Li, Z.Y., Su, Z.B., Chen, E.X., Li, X., Li, L.H., Wang, X. F., Pan, X.D., Gao, L.S., Han, Z.B., 2017. Modeling forest above-ground biomass dynamics using multi-source data and incorporated models: a case study over the Qilian mountains. *Agric. For. Meteorol.* 246, 1–14. <https://doi.org/10.1016/j.agrformet.2017.05.026>.
- Wagner, B., Liang, E.Y., Li, X.X., Dulamsuren, C., Leuschner, C., Hauck, M., 2015. Carbon pools of semi-arid *Picea crassifolia* forests in the Qilian Mountains (north-eastern Tibetan plateau). *Forest Ecol. Manag.* 343, 136–143. <https://doi.org/10.1016/j.foreco.2015.02.001>.
- Wang, C., Wang, X.B., Liu, D.W., Wu, H.H., Lü, X.T., Fang, Y.T., Cheng, W.X., Luo, W.T., Jiang, P., Shi, J.S., Yin, H.Q., Zhou, J.Z., Han, X.G., Bai, E., 2014. Aridity threshold in controlling ecosystem nitrogen cycling in arid and semi-arid grasslands. *Nat. Commun.* 5, 4799. <https://doi.org/10.1038/ncomms5799>.
- Wang, J., Wang, G.X., Wang, C.T., Ran, F., Chang, R.Y., 2016. Carbon storage and potentials of the broad-leaved forest in alpine region of the Qinghai-Xizang Plateau, China. *Chin. J. Plant Ecol.* 40 (4), 374–384. <https://doi.org/10.17521/cjpe.2015.0152>.
- Wang, B., Yu, P.T., Yu, Y.P., Wan, Y.F., Wang, Y.H., Zhang, L., Wang, S.L., Wang, X., Liu, Z.B., Xu, L.H., 2020. Effects of canopy position on climate-growth relationships of Qinghai spruce in the central Qilian mountains, northwestern China. *Dendrochronologia* 65, 125756. <https://doi.org/10.1016/j.dendro.2020.125756>.
- Woodbury, P.B., Smith, J.E., Heath, L.S., 2007. Carbon sequestration in the U.S. forest sector from 1990 to 2010. *Forest Ecol. Manag.* 241, 14–27. <https://doi.org/10.1016/j.foreco.2006.12.008>.
- Wu, G.J., Liu, X.H., Chen, T., Xu, G.B., Wang, W.Z., Zeng, X.M., Zhang, X.W., 2015. Elevation-dependent variations of tree growth and intrinsic water-use efficiency in Schrenk spruce (*Picea schrenkiana*) in the western Tianshan Mountains, China. *Front. Plant Sci.* 6, 309. <https://doi.org/10.3389/fpls.2015.00309>.
- Xia, J., Ning, L.K., Wang, Q., Chen, J.X., Wan, L., Hong, S., 2017. Vulnerability of and risk to water resources in arid and semi-arid regions of West China under a scenario of climate change. *Clim. Change* 144, 549–563. <https://doi.org/10.1007/s10584-016-1709-y>.
- Xu, Z.L., Zhao, C.Y., Feng, Z.D., Zhang, F., Sher, H., Wang, C., Peng, H.H., Wang, Y., Zhao, Y., Wang, Y., Peng, S.Z., Zheng, X.L., 2013. Estimating realized and potential carbon storage benefits from reforestation and afforestation under climate change: a case study of the Qinghai spruce forests in the Qilian Mountains, northwestern China. *Mitig. Adapt. Strat. GL* 18 (8), 1257–1268. <https://doi.org/10.1007/s11027-012-9420-4>.
- Xu, B., Yang, Y.H., Li, P., Shen, H.H., Fang, J.Y., 2014. Global patterns of ecosystem carbon flux in forest: biometric databased synthesis. *Global Biogeochem. Cycles* 28, 962–973. <https://doi.org/10.1002/2013GB004593>.
- Yang, B., He, M.H., Shishov, V., Tychkov, I., Vaganov, E., Rossi, S., Ljungqvist, F.C., Bräunin, A., Griebinger, J., 2017. New perspective on spring vegetation phenology and global climate change based on Tibetan Plateau tree-ring data. *Proc. Natl. Acad. Sci. U. S. A.* 114 (27), 6966–6971. <https://doi.org/10.1073/pnas.1616608114>.
- Yang, H.J., Gou, X.H., Yin, D.C., Du, M.M., Liu, L.Y., Wang, K., 2022. Research on the coordinated development of ecosystem services and well-being in agricultural and pastoral areas. *J. Environ. Manage.* 304, 114300. <https://doi.org/10.1016/j.jenvman.2021.114300>.
- Zeng, W.S., Tomppo, E., Healey, S.P., Gadow, K.V., 2015. The national forest inventory in China: history - results - international context. *For. Ecosyst.* 2, 23. <https://doi.org/10.1186/s40663-015-0047-2>.
- Zeng, W.S., Li, L.Q., Xiao, Q.H., Dang, Y.F., Ma, K.X., Sun, J.L., Wang, X.J., Li, Z.H., Feng, Q., Yang, X.Y., Li, G.X., Qi, H., Gong, W.C., Bai, W.G., 2016. LY/T 2655–2016 Tree biomass models and related parameters to carbon accounting for *Picea*. <https://hbba.sacinfo.org.cn/stdDetail/0c369963308d301b9e9216fa4c94a4be>.
- Zhang, P.C., Shao, G.F., Zhao, G., Le Master, D.C., Parker, G.R., Dunning, J.B., Li, Q.L., 2000. China's forest policy for the 21st century. *Science* 288, 2135–2136. <https://doi.org/10.1126/science.288.5474.2135>.
- Zhang, C.H., Ju, W.M., Chen, J.M., Zan, M., Li, D.Q., Zhou, Y.L., Wang, X.Q., 2013. China's forest biomass carbon sink based on seven inventories from 1973 to 2008. *Clim. Change* 118, 933–948. <https://doi.org/10.1007/s10584-012-0666-3>.
- Zhang, C.H., Ju, W.M., Chen, J.M., Wang, X.Q., Yang, L., Zheng, G., 2015. Disturbance induced reduction of biomass carbon sinks of China's forests in recent years. *Environ. Res. Lett.* 10, 114021. <https://doi.org/10.1088/1748-9326/10/11/114021>.
- Zhang, J.Z., Ross Alexander, M., Gou, X.H., Deslauriers, A., Fonti, P., Zhang, F., Pederson, N., 2020a. Extended xylogenesis and stem biomass production in *Juniperus przewalskii* Kom. during extreme late-season climatic events. *Ann. For. Sci.* 77, 99. <https://doi.org/10.1007/s13595-020-01008-1>.
- Zhang, Y.X., Yan, H.W., Huang, G.S., Zeng, W.S., Dang, Y.F., Yang, X.Y., Chen, X.Y., Nie, X.Y., Ma, K.X., Chen, Z.X., Zhang, C.C., 2020. GB/T 38590–2020 Technical Regulations for Continuous Forest Inventory. Standards Press of China, Beijing. <https://openstd.samr.gov.cn/bzgk/gb/newGbInfo?hcno=AA97E70AF9F27615D087CBC56A9817CD>.
- Zhang, J.Z., Gou, X.H., Alexander, M.R., Xia, J.Q., Wang, F., Zhang, F., Man, Z.H., Pederson, N., 2021. Drought limits wood production of *Juniperus przewalskii* even as growing seasons lengthens in a cold and arid environment. *Catena* 196, 104936. <https://doi.org/10.1016/j.catena.2020.104936>.
- Zhang, H.Y., Feng, Z.K., Shen, C.Y., Li, Y.D., Feng, Z.M., Zeng, W.S., Huang, G.S., 2022. Relationship between the geographical environment and the forest carbon sink capacity in China based on an individual-tree growth-rate model. *Ecol. Indic.* 138, 108814. <https://doi.org/10.1016/j.ecolind.2022.108814>.
- Zhang, J.Z., Gou, X.H., Rademacher, T., Wang, L.Y., Li, Y.L., Sun, Q.P., Wang, F., Cao, Z. Y., 2023. Interaction of age and elevation on xylogenesis in *Juniperus przewalskii* in a cold and arid region. *Agric. For. Meteorol.* 337, 109480. <https://doi.org/10.1016/j.agrformet.2023.109480>.
- Zhao, M.M., Yang, J.L., Zhao, N., Liu, Y., Wang, Y.F., Wilson, J.P., Yue, T.X., 2019. Estimation of China's forest stand biomass carbon sequestration based on the continuous biomass expansion factor model and seven forest inventories from 1977 to 2013. *Forest Ecol. Manag.* 448, 528–534. <https://doi.org/10.1016/j.foreco.2019.06.036>.
- Zhao, Y.H., Gao, C.C., Rong, Z.L., Zhao, C.Y., 2020. Understorey vegetation should not be ignored in the estimation of forest carbon stocks in Qilian Mountains National Nature Reserve. *Acta Ecol. Sin.* 41 (4), 318–324. <https://doi.org/10.1016/j.chnaes.2020.06.009>.
- Zhao, M.M., Yang, J.L., Zhao, N., Xiao, X.M., Yue, T.X., Wilson, J.P., 2021. Estimation of the relative contributions of forest area expansion and growth to China's forest stand biomass carbon sequestration from 1977 to 2018. *J. Environ. Manage.* 300, 113757. <https://doi.org/10.1016/j.jenvman.2021.113757>.
- Zhou, Y., Hao, F.H., Meng, W., Fu, J.F., 2014. Scenario analysis of energy-based low-carbon development in China. *J. Environ. Sci.* 26 (8), 1631–1640. <https://doi.org/10.1016/j.jes.2014.06.003>.